

ECE 795:
Quantitative
Electrophysiology

Notes for Lecture #2

Wednesday, September 20, 2006

3. CELL EXCITABILITY

Here we will look at the response of the cell membrane to current injections and changes in the transmembrane potential.

The key features are:

1. the *linear* behaviour around the resting membrane potential, and
2. the *nonlinear* behaviour that leads to the generation of “action potentials”.

Equivalent circuit near rest:

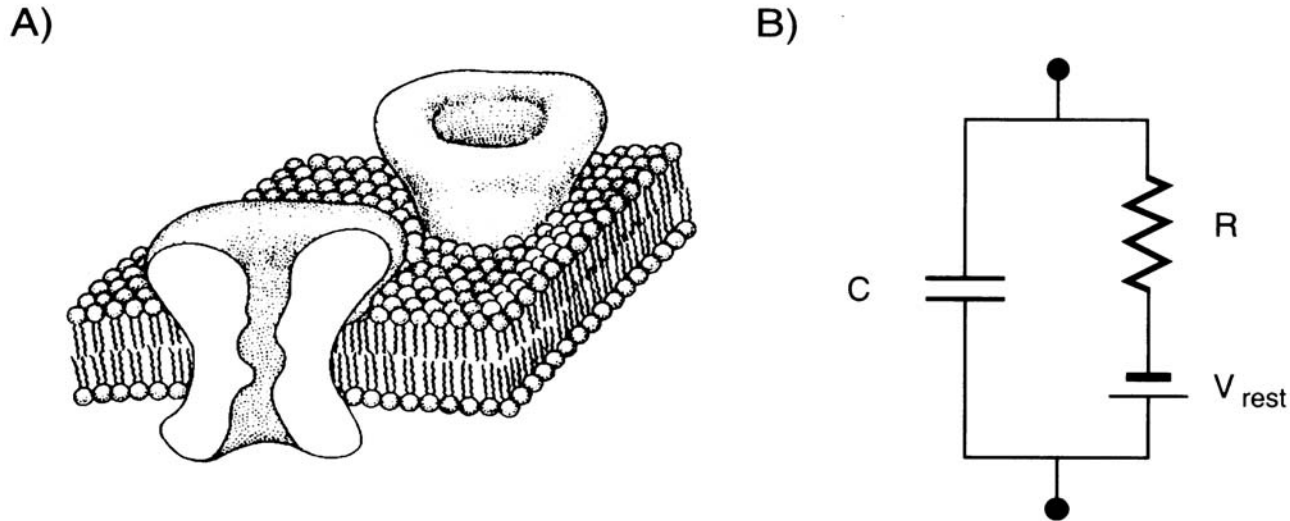


Fig. 1.1 NATURE OF THE PASSIVE NEURONAL MEMBRANE (A) Schematic representation of a small patch of membrane of the types enclosing all cells. The 30–50 Å thin bilayer of lipids isolates the extracellular side from the intracellular one. From an electrical point of view, the resultant separation of charge across the membrane acts akin to a capacitance. Proteins inserted into the membrane, here ionic channels, provide a conduit through the membrane. Reprinted by permission from Hille (1992). (B) Associated lumped electrical circuit for this patch, consisting of a capacitance and a resistance in series with a battery. The resistance mimics the behavior of voltage-independent ionic channels inserted throughout the membrane and the battery accounts for the cell's resting potential V_{rest} .

(from Koch)

Notation for potentials:

- Transmembrane potential:

$$V_m = \Phi_i - \Phi_e$$

- Membrane potential relative to rest:

$$v_m = V_m - V_{\text{rest}}$$

- Intra- and extra-cellular potentials relative to their respective baseline values:

$$\phi_i = \Phi_i - \Phi_{i,\text{rest}}$$

$$\phi_e = \Phi_e - \Phi_{e,\text{rest}}$$

Spherical cell response to current step:

If R_m ($\Omega \cdot \text{cm}^2$) and C_m ($\mu\text{F} / \text{cm}^2$) are the *specific resistance* and the *specific capacitance*, respectively, of the membrane, then for a spherical cell with surface area A (cm^2) the *membrane resistance* is:

$$R = \frac{R_m}{A} \quad \Omega, \quad (7.1)$$

and the *membrane capacitance* is:

$$C = C_m A \quad \mu\text{F}. \quad (7.2)$$

Spherical cell response to current step (cont.):

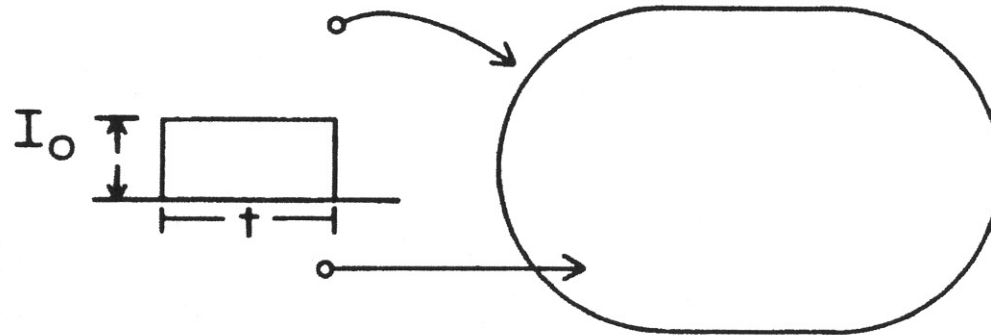


Figure 7.1. A current step is applied between an intracellular and extracellular microelectrode. The cell shape is roughly spherical.

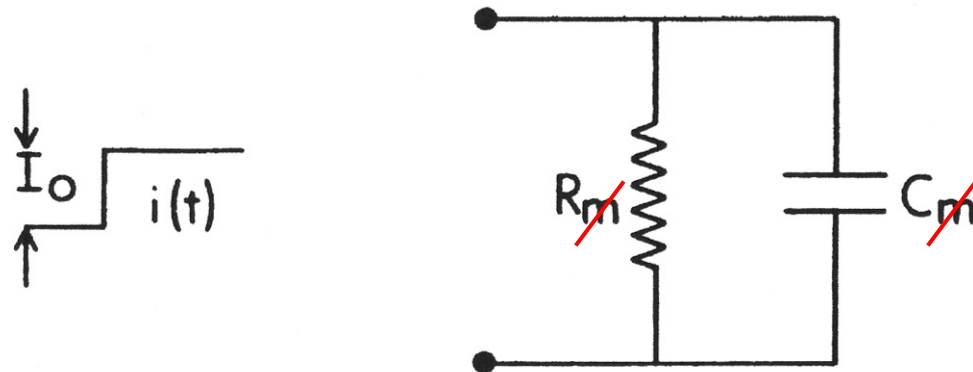


Figure 7.2. Equivalent electrical circuit for preparation described in Fig. 7.1.

Spherical cell response to current step (cont.):

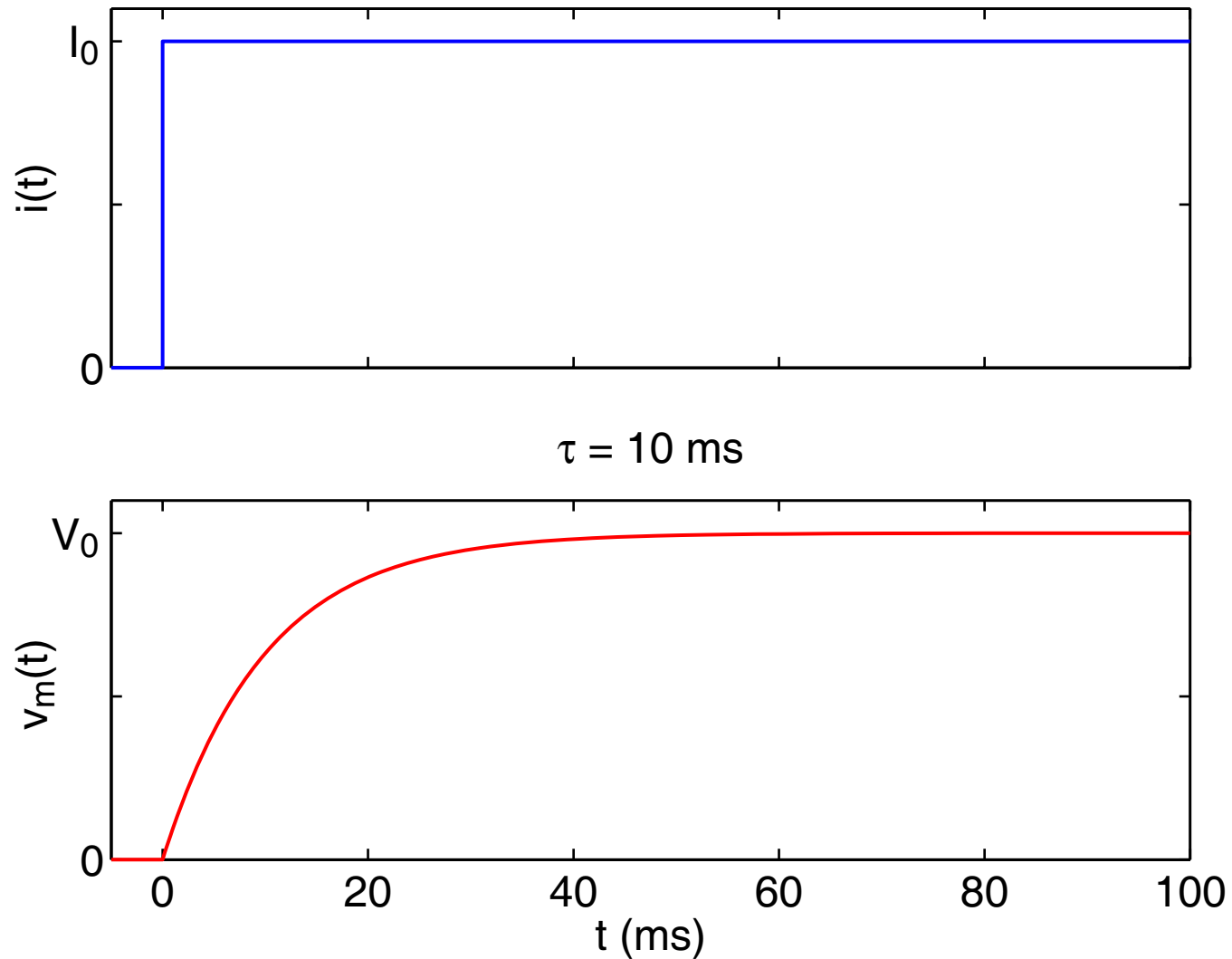
The response of the relative transmembrane potential v_m of a spherical cell subjected to an intracellularly-injected current step of amplitude I_0 is:

$$v_m = I_0 R \left(1 - e^{-t/\tau} \right) \quad (7.3)$$

$$= V_0 \left(1 - e^{-t/\tau} \right), \quad (7.4)$$

where $\tau = RC$ and $V_0 = I_0 R = v_m(t \rightarrow \infty)$.

Spherical cell response to current step (cont.):



Strength-duration relationship:

Suppose that a relative transmembrane potential of V_T ($< V_0$) is the “threshold” potential for eliciting an action potential.

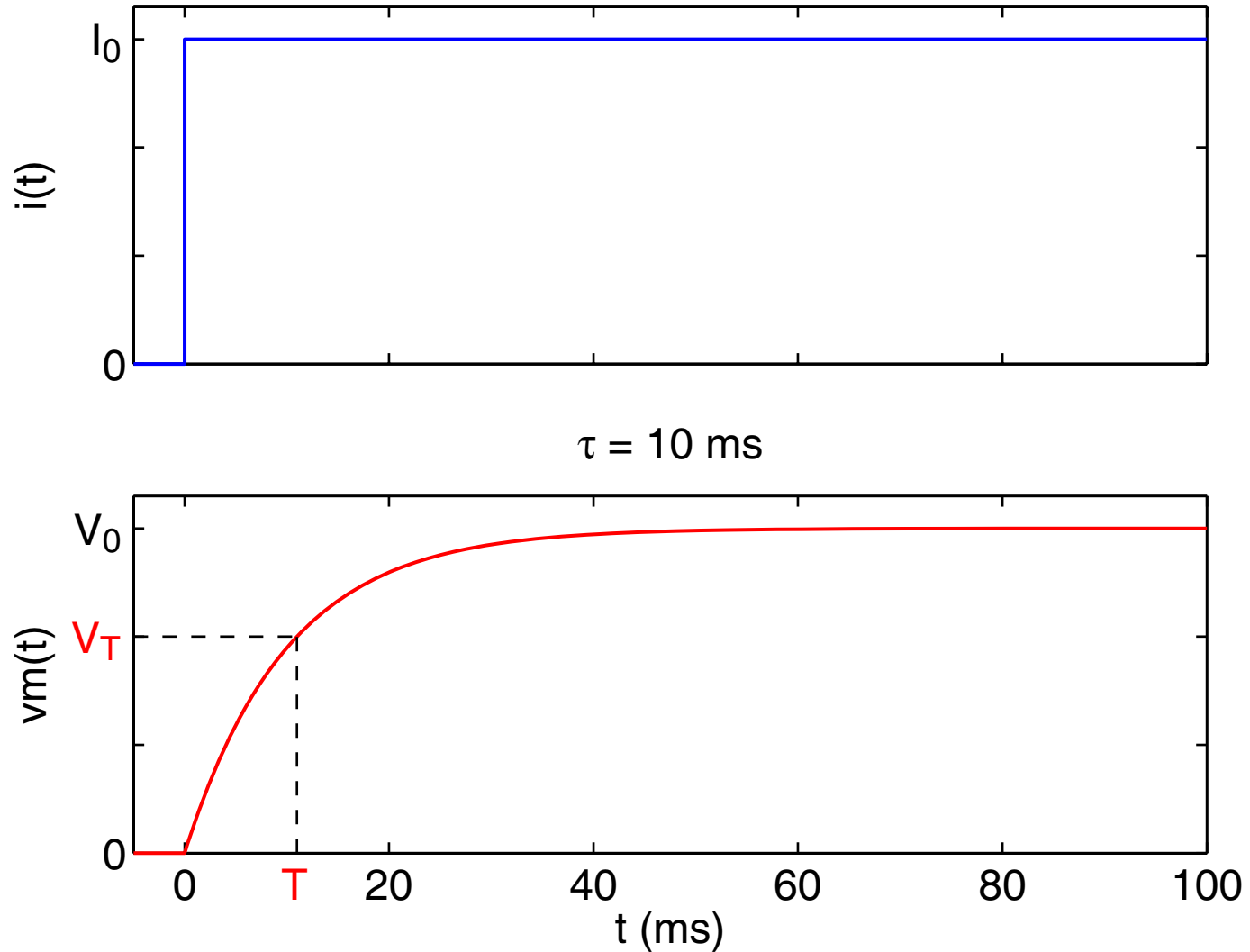
From Eqn. (7.4), the membrane potential will reach V_T at time T (following the onset of the current pulse) according to the equation:

$$V_T = V_0 \left(1 - e^{-T/\tau} \right).$$

Solving for T gives:

$$T = -\tau \ln \left(1 - \frac{V_T}{V_0} \right).$$

Strength-duration relationship (cont.):



Strength-duration relationship (cont.):

A strength-duration curve is obtained by plotting:

$$V_0 = V_T / \left(1 - e^{-T/\tau}\right) \quad (7.5)$$

for a fixed value of V_T .

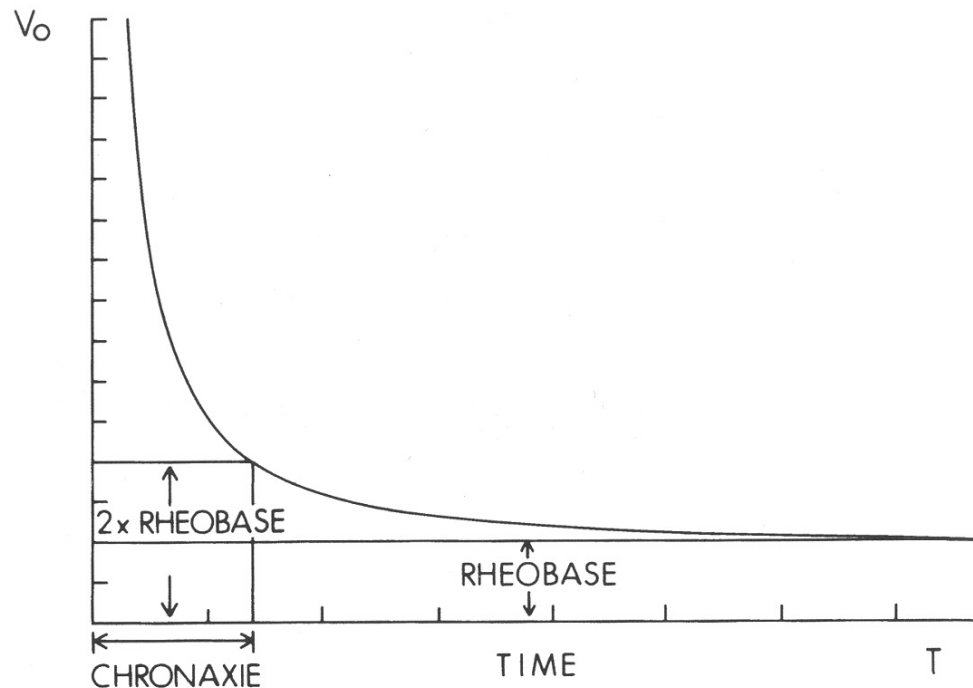


Figure 7.3. Strength-duration curve [from Eq. 7.5].

Strength-duration relationship (cont.):

- *Rheobase* is the minimum excitation required to just reach threshold as $T \rightarrow \infty$, i.e., $V_0 = V_T$.
- *Chronaxie* is the pulse duration T_c required to reach threshold when the stimulus is twice rheobase, which can be calculated according to:

$$T_c = \tau \ln 2 = 0.693\tau. \quad (7.8)$$

Chronaxie is significant as a nominal time period required to reach the threshold voltage.

Action potentials are:

- *all-or-nothing* events,
- *regenerative*,
- generated when a *threshold* is reached,
- *propagating* potentials, and
- also known as nerve *spikes* or *impulses*.

Transmembrane action potential morphology:

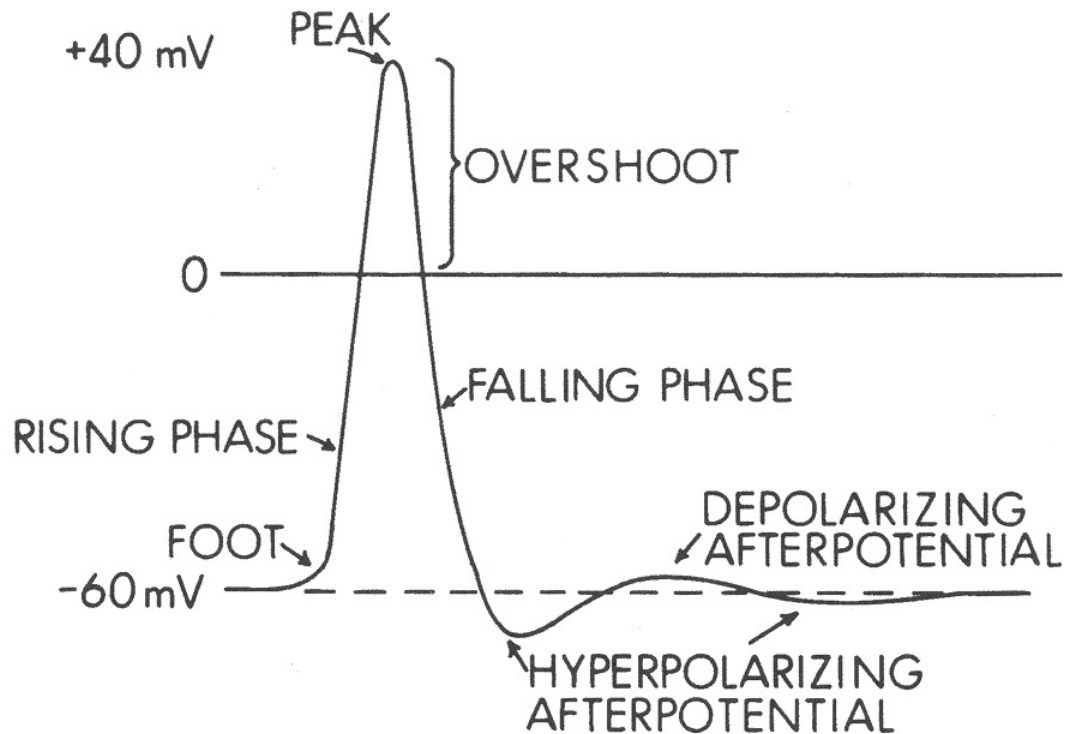


Figure 5.4. Diagram to show the nomenclature applied to an action potential and the afterpotentials that may follow it.

Observing action potentials (cont.):

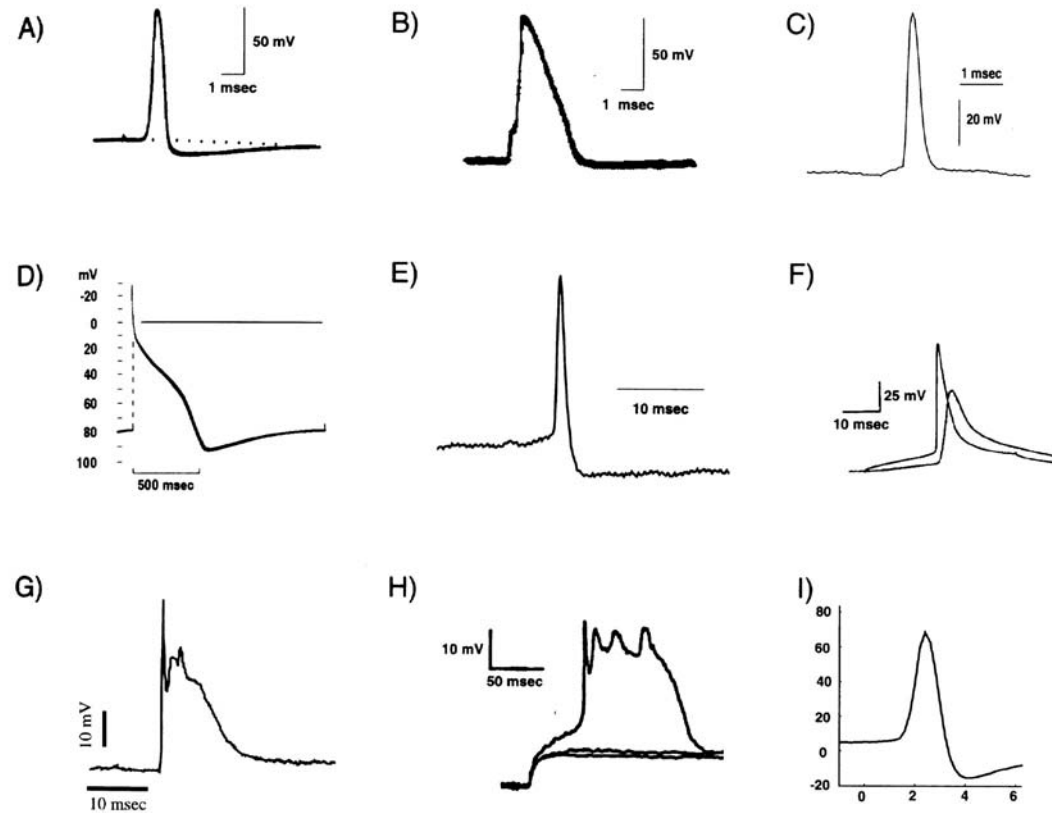


Fig. 6.1 ACTION POTENTIALS OF THE WORLD Action potentials in different invertebrate and vertebrate preparations. Common to all is a threshold below which no impulse is initiated, and a stereotypical shape that depends only on intrinsic membrane properties and not on the type or the duration of the input. (A) Giant squid axon at 16° C. Reprinted by permission from Baker, Hodgkin, and Shaw (1962). (B) Axonal spike from the node of Ranvier in a myelinated frog fiber at 22° C. Reprinted by permission from Dodge (1963). (C) Cat visual cortex at 37° C. Unpublished data from J. Allison, printed with permission. (D) Sheep heart Purkinje fiber at 10° C. Reprinted by permission from Weidmann (1956). (E) Patch-clamp recording from a rabbit retinal ganglion cell at 37° C. Unpublished data from F. Amthor, printed with permission. (F) Layer 5 pyramidal cell in the rat at room temperatures. Simultaneous recordings from the soma and the apical trunk. Reprinted by permission from Stuart and Sakmann (1994). (G) A complex spike—consisting of a large EPSP superimposed onto a slow dendritic calcium spike and several fast somatic sodium spikes—from a Purkinje cell body in the rat cerebellum at 36° C. Unpublished data from D. Jaeger, printed with permission. (H) Layer 5 pyramidal cell in the rat at room temperature. Three dendritic voltage traces in response to three current steps of different amplitudes reveal the all-or-none character of this slow event. Notice the fast superimposed spikes. Reprinted by permission from Kim and Connors (1993). (I) Cell body of a projection neuron in the antennal lobe in the locust at 23° C. Unpublished data from G. Laurent, printed with permission.

(from Koch)

Nonlinear membrane behaviour:

Subthreshold and action potential responses to a brief stimulating current.

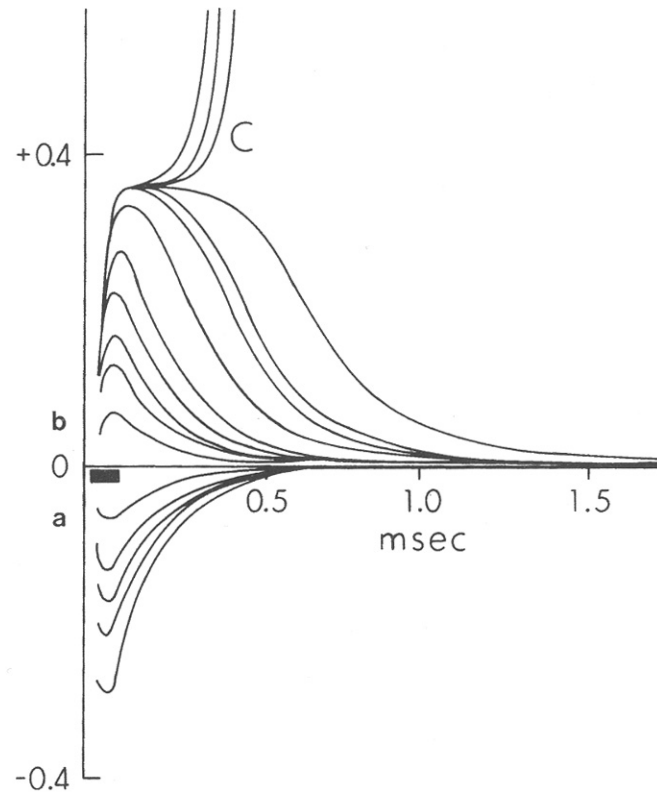


Figure 5.5. Subthreshold responses recorded extracellularly from a crab axon in the vicinity of the stimulating electrodes. The axon was placed in paraffin oil, and, consequently the measured extracellular potential is directly related to the transmembrane potential (according to the linear core-conductor model described in Chapter 6). The heavy bar indicates the stimulus period, which was approximately 50 μ sec in duration. The ordinate is a voltage scale on which the height of the action potential is taken as one unit. [From A. L. Hodgkin, The subthreshold potentials in a crustacean nerve fibre, *Proc. R. Soc. London, Ser. B* **126**:87–121 (1938).]

Nonlinear membrane behaviour (cont.):

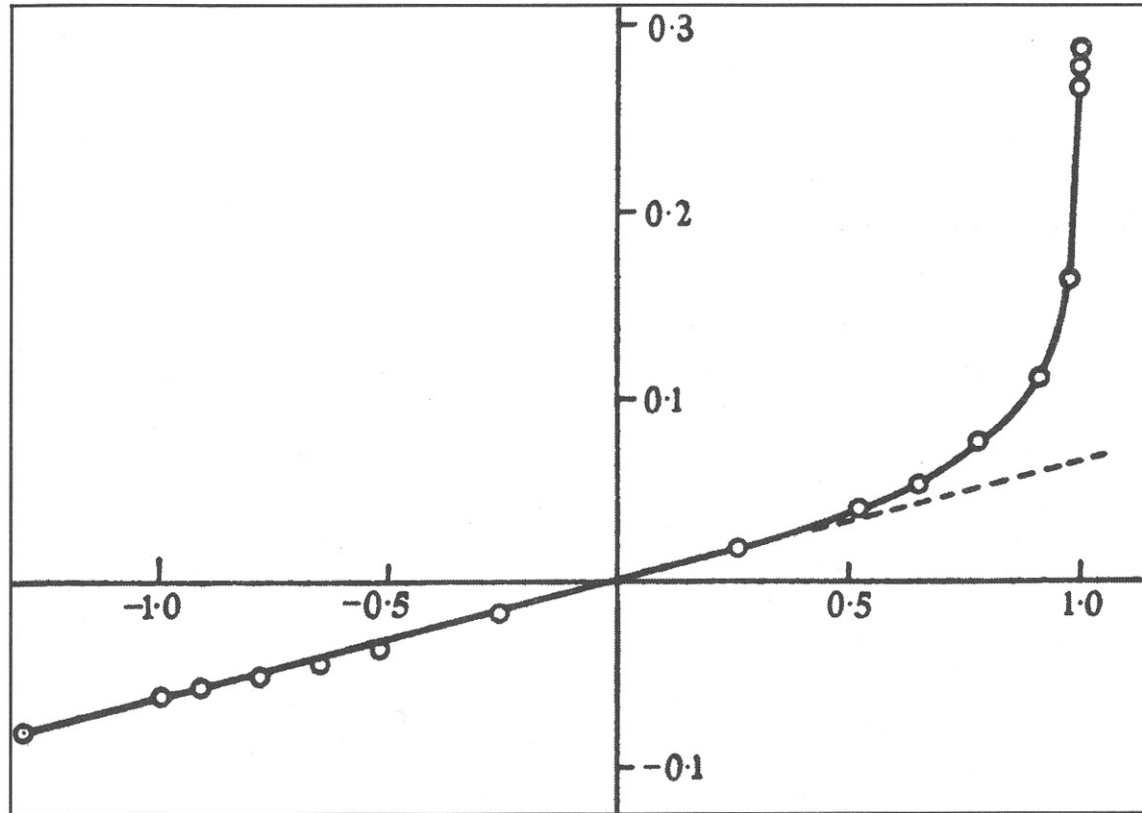


Figure 5.6. The relation between stimulus and response in a crab axon. This figure was derived from Fig. 5.5. The abscissa shows the stimulus intensity, measured as a fraction of the threshold stimulus. The ordinate shows the recorded potential 0.29 msec after the stimulus, measured as a fraction of the action potential peak. [Reprinted with permission from A. L. Hodgkin, The subthreshold potentials in a crustacean nerve fibre, *Proc. R Soc. London, Ser. B* 126:87–121 (1938).]

Nonlinear membrane behaviour (cont.):

For the squid axon:-

- $C_m \approx 1 \mu\text{F}/\text{cm}^2$ throughout the entire action potential
- $R_m \approx 1000 \Omega \cdot \text{cm}^2$ at rest
- $R_m \approx 25 \Omega \cdot \text{cm}^2$ at the peak of the action potential

Origin of action potential, resting and peak voltages:

In the classic studies by Hodgkin and Huxley, the results were related to the Goldman-Hodgkin-Katz (GHK) equation for the transmembrane potential:

$$V_m = \frac{RT}{F} \ln \left[\frac{P_K [K]_e + P_{Na} [Na]_e + P_{Cl} [Cl]_i}{P_K [K]_i + P_{Na} [Na]_i + P_{Cl} [Cl]_e} \right], \quad (5.1)$$

where P_p is the *permeability* of the p^{th} ion channel.

Origin of action potential, resting and peak voltages (cont.):

As we have observed previously, the **resting transmembrane potential** is slightly higher than the **potassium equilibrium potential**.

Looking at the action potential waveform, we see that the **peak transmembrane potential** approaches but never exceeds the **sodium equilibrium potential**.

Origin of action potential, resting and peak voltages (cont.):

This result is consistent with an elevated sodium permeability in the rising phase and peak of the action potential.

Good agreement between theory and experimental data from the squid axon is obtained with:

$P_K:P_{Na}:P_{Cl} = 1.0:0.04:0.45$ for membrane
at rest

$P_K:P_{Na}:P_{Cl} = 1.0:20.0:0.45$ at an action
potential peak

Origin of action potential, resting and peak voltages (cont.):

To a first approximation:

$$\text{At rest: } V_m \approx E_K = \frac{RT}{F} \ln \left(\frac{[K]_e}{[K]_i} \right) \quad (5.3)$$

$$\text{At the peak: } V_m \approx E_{Na} = \frac{RT}{F} \ln \left(\frac{[Na]_e}{[Na]_i} \right) \quad (5.4)$$

Origin of action potential, resting and peak voltages (cont.):

In an experiment using radioactive tracers, it was found for the cuttlefish *Sepia* giant axon that:

- at rest, there is steady influx of sodium and efflux of potassium, consistent with $E_K < V_{\text{rest}} < E_{\text{Na}}$
- during an action potential there is an influx of 3.7 pmoles/cm² of sodium
- during an action potential there is an efflux of 4.3 pmoles/cm² of potassium

Origin of action potential, resting and peak voltages (cont.):

These results can be compared with the charge movement required to depolarize the transmembrane potential by around 125 mV:

$$\begin{aligned} Q &= CV = 1.0 \times 10^{-6} \times 0.125 \\ &= 1.25 \times 10^{-7} \text{ C/cm}^2 \end{aligned}$$

$$\begin{aligned} \Rightarrow \text{number of mole} &= Q/F \\ &= 1.25 \times 10^{-7} / 96487 \\ &= 1.3 \text{ pmol/cm}^2 \end{aligned}$$

4. INTRODUCTION TO THE HODGKIN-HUXLEY MODEL

Based on a set of detailed physiological experiments, Hodgkin & Huxley developed a nonlinear dynamical model of the excitable cell membrane. Their formulation for gating dynamics is the basis of almost all subsequent biophysical models of excitable cell membranes.

Voltage and space clamp:

- Hodgkin and Huxley used a *voltage and space clamp* apparatus to measure and quantify ionic currents in the squid giant axon.
- By applying a *voltage clamp* and making discrete steps in transmembrane voltage, the capacitive current is absent, and consequently only the ionic currents are recorded.
- By inserting a conducting wire along the inside of the axon, a *space clamp* is applied, i.e., the intracellular potential is the same along the entire length of the axon. Consequently, the ionic current from a large number of ion channels is recorded.

Voltage and space clamp (cont.):

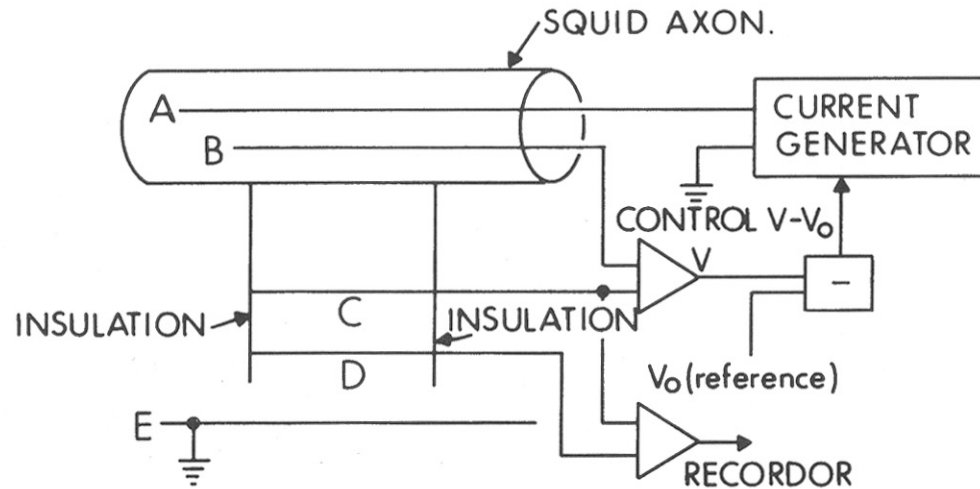


Figure 5.7. Schematic diagram showing the voltage and space clamp apparatus as developed by Hodgkin, Huxley, and Katz [6]. Current electrodes are (A) and (E); potential sensing electrodes are (B) and (C). Transmembrane current is determined from the potential between (C) and (D) and the total resistance between these electrodes. (Since the membrane current is uniform and in the radial direction only, the resistance can be calculated if the electrode end-effects are neglected.) Transmembrane voltage V is compared with the desired clamp V_0 , and the difference causes a proportional transmembrane current of proper sign so that $(V - V_0) \rightarrow 0$.

Example net ionic current to a voltage step:

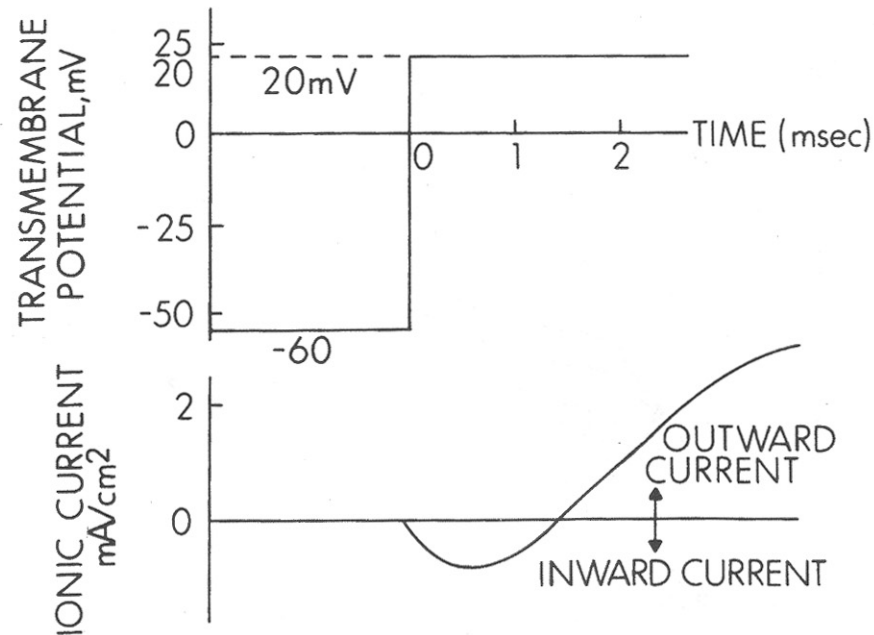


Figure 5.8. Illustrative example of the ionic current for a squid axon assuming the application of a voltage clamp of $V_m = 20$ mV at $t = 0$ sec. The assumed parameters are: resting potential of $V_m = V_{\text{rest}} = -60$ mV; sodium and potassium Nernst potentials $E_K = -70$ mV and $E_{\text{Na}} = 57$ mV.

Measured ionic current for different voltage steps:

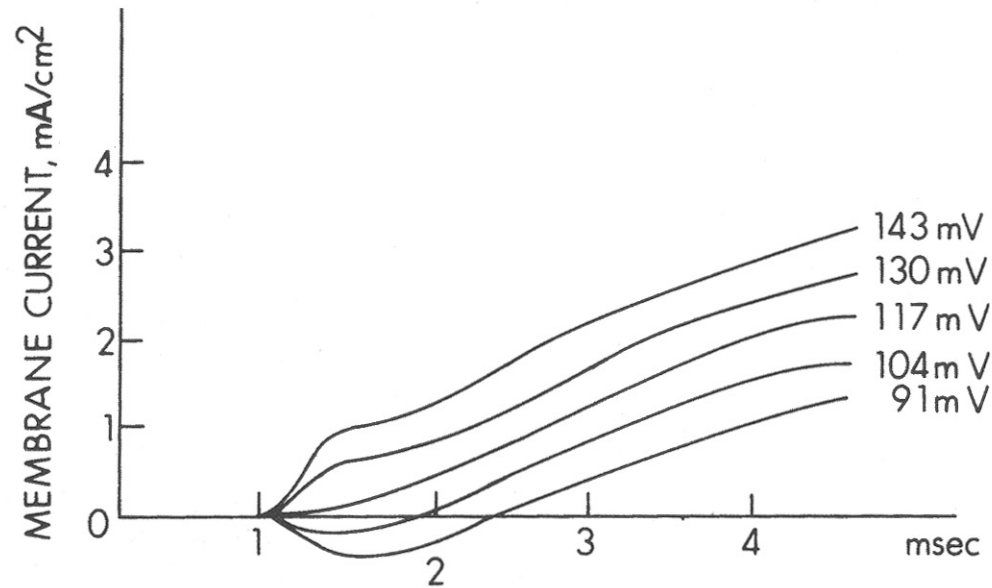


Figure 5.9. Measured ionic current for the squid axon following the application of a voltage clamp of the value indicated. The sodium Nernst potential is reached with a step change of 117 mV (since the resting potential is -60 mV and $E_{\text{Na}} = 57$ mV). [From A. L. Hodgkin, Ionic movements and electrical activity in giant nerve fibers, *Proc. R. Soc.* **148**:1–37 (1958). After A. L. Hodgkin, A. F. Huxley, and B. Katz, Measurement of current voltage relations in the membrane of the giant axon of *Loligo*, *J. Physiol.* **116**:424–448 (1952).]

Current-voltage curves:

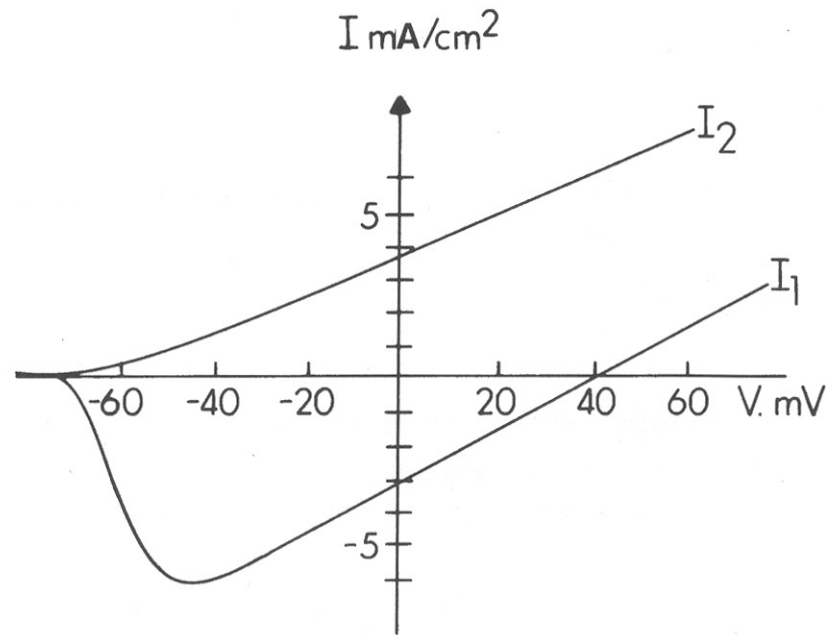


Figure 5.10. A typical current–voltage relation for squid axon. Curve I_1 shows the peak inward current versus clamped transmembrane voltage V_m after holding at rest. Curve I_2 plots the steady-state outward current versus the clamped voltage V_m . The voltage clamp value of V_m is plotted on the abscissa. Note that $I_1 = 0$ at $V_m = V_{\text{rev}} \approx E_{\text{Na}}$.

Separation of sodium and potassium currents:

Hodgkin and Huxley utilized two approaches to separating the contributions of sodium and potassium currents to the net ionic current:

1. Assuming $I_K = 0$ for $0 \leq t \leq T/3$, where T is the time of peak inward current.
2. Varying the extracellular sodium concentration while keeping the extracellular potassium concentration fixed.

Effects of varying extracellular sodium concentration:

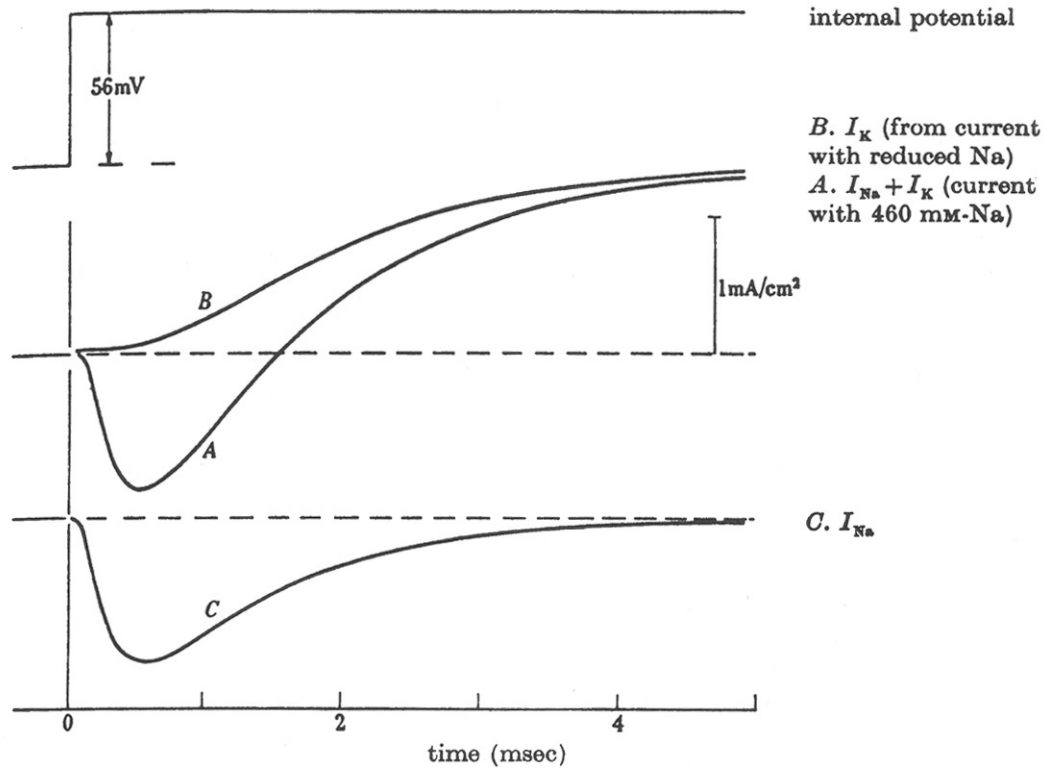


Figure 5.11. Analysis of the ionic current in a *Loligo* axon during a voltage clamp. Trace A shows the response to a depolarization of 56 mV with the axon in seawater. Trace B is the response with the axon in a solution comprising 10% seawater and 90% isotonic choline chloride solution. Trace C is the difference between traces A and B. Normal $E_{Na} = 57$ mV and in the reduced seawater $E_{Na} = -1$ mV. [From A. L. Hodgkin, Ionic movements and electrical activity in giant nerve fibers, *Proc. R. Soc.* **148**:1-37 (1958). After A. L. Hodgkin, A. F. Huxley, and B. Katz, Measurement of current voltage relations in the membrane of the giant axon of *Loligo*, *J. Physiol.* **116**:424-448 (1952).]

Ionic conductances from ionic currents:

Rearranging Eqns. (3.26) and (3.27) gives:

$$g_{\text{K}}(t) = \frac{I_{\text{K}}(t)}{(V_m - E_{\text{K}})}, \quad (5.11)$$

$$g_{\text{Na}}(t) = \frac{I_{\text{Na}}(t)}{(V_m - E_{\text{Na}})}. \quad (5.12)$$

In the voltage clamp experiments, the denominators of Eqns. (5.11) and (5.12) are constant \Rightarrow

$$g_{\text{K}}(t) \propto I_{\text{K}}(t), \quad g_{\text{Na}}(t) \propto I_{\text{Na}}(t).$$

Ionic conductances from ionic currents (cont.):

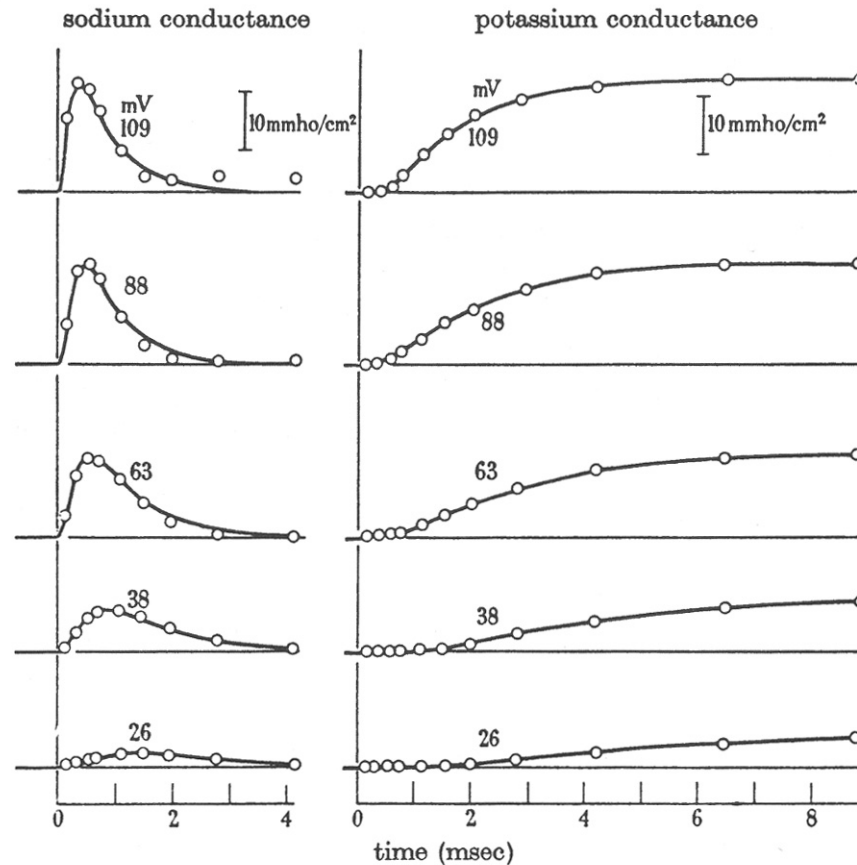


Figure 5.12. Conductance changes brought about by clamped depolarizations of different magnitudes. The circles represent values derived from the experimental measurements of ionic current, and the curves are drawn according to methods described in the text. The voltage clamp transmembrane potential values are in millivolts and are described relative to the resting value (i.e., v_m). [From A. L. Hodgkin, Ionic movements and electrical activity in giant nerve fibers, *Proc. R. Soc.* **148**:1–37 (1958). After A. L. Hodgkin and A. F. Huxley, A quantitative description of membrane current and its application to conduction and excitation in nerve. *J. Physiol.* **117**:500–544 (1952).]

Hodgkin-Huxley equations:

Potassium channel model:

- Potassium conductance:

$$g_K(t, v_m) = \bar{g}_K n^4(t, v_m) \quad (5.13)$$

- Potassium *activation* particle dynamics:

$$\frac{dn(t, v_m)}{dt} = \alpha_n(v_m) (1 - n) - \beta_n(v_m) n \quad (5.14)$$

or:

$$\frac{dn(t, v_m)}{dt} = \frac{n_\infty - n}{\tau_n} \quad (5.17)$$

Hodgkin-Huxley equations (cont.):

➤ Potassium *activation* transition rates:

$$\alpha_n(v_m) = \frac{0.01 (10 - v_m)}{\exp\left(\frac{10 - v_m}{10}\right) - 1} \quad (5.19)$$

$$\beta_n(v_m) = 0.125 \exp\left(\frac{-v_m}{80}\right) \quad (5.20)$$

Hodgkin-Huxley equations:

Sodium channel model:

- Sodium conductance:

$$g_{\text{Na}}(t, v_m) = \bar{g}_{\text{Na}} m^3(t, v_m) h(t, v_m) \quad (5.21)$$

- Sodium *activation* particle dynamics:

$$\frac{dm(t, v_m)}{dt} = \alpha_m(v_m) (1 - m) - \beta_m(v_m) m \quad (5.22)$$

- Sodium *inactivation* particle dynamics:

$$\frac{dh(t, v_m)}{dt} = \alpha_h(v_m) (1 - h) - \beta_h(v_m) h \quad (5.23)$$

Hodgkin-Huxley equations (cont.):

- Sodium *activation* transition rates:

$$\alpha_m(v_m) = \frac{0.1(25 - v_m)}{\exp\left(\frac{25 - v_m}{10}\right) - 1};$$
$$\beta_m(v_m) = 4 \exp\left(\frac{-v_m}{18}\right) \quad (5.31)$$

- Sodium *inactivation* transition rates:

$$\alpha_h(v_m) = 0.07 \exp\left(\frac{-v_m}{20}\right);$$
$$\beta_h(v_m) = \left\{ \exp\left(\frac{30 - v_m}{10}\right) + 1 \right\}^{-1} \quad (5.32)$$

Hodgkin-Huxley equations (cont.):

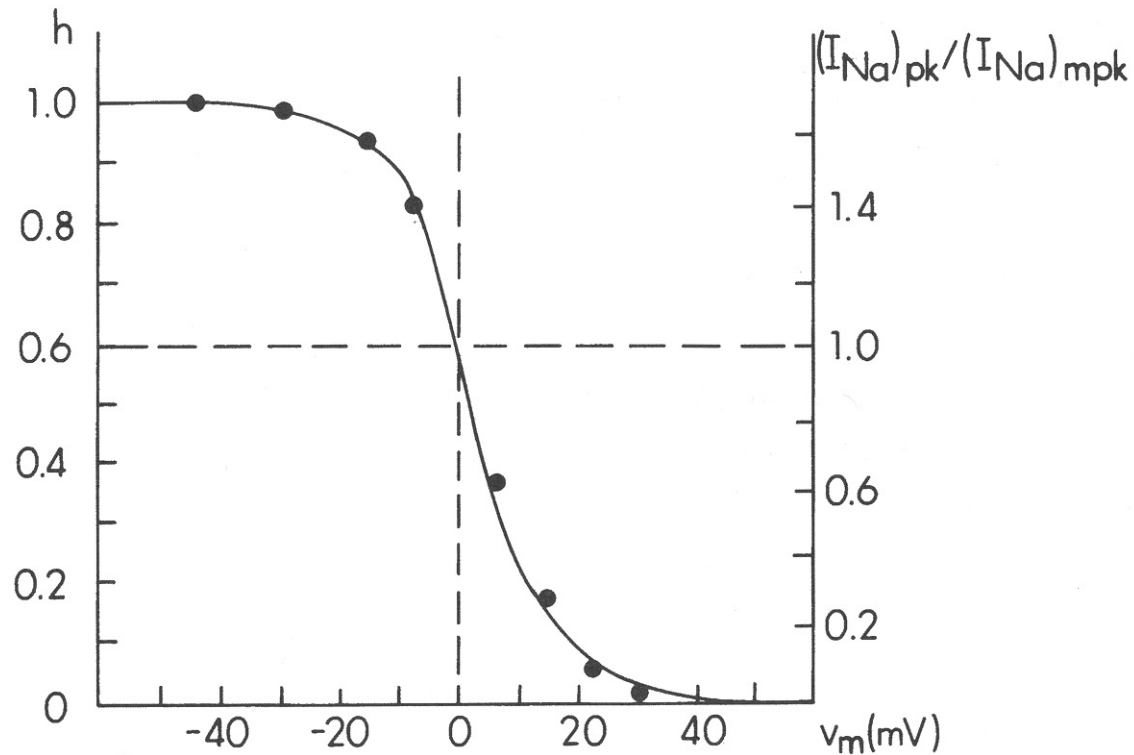


Figure 5.13. Sodium inactivation curve. Abscissa is the deviation from the resting potential (i.e., v_m). Dots are experimental points, and the smooth curve satisfies (5.33) for $v_{mh} = 2.5$ mV. [From A. L. Hodgkin and A. F. Huxley, The dual effect of membrane potential on sodium conductance in the giant axon of *Loligo*. *J. Physiol.* **116**:497–506 (1952).]

Hodgkin-Huxley equations (cont.):

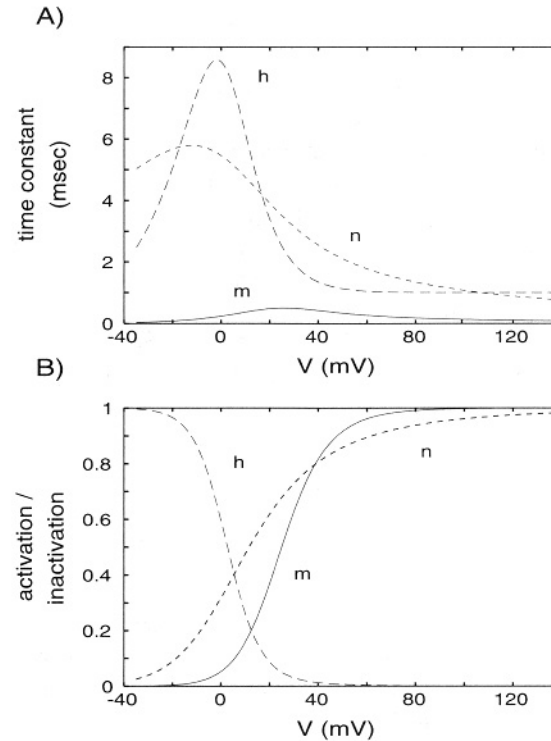


Fig. 6.3 VOLTAGE DEPENDENCY OF THE GATING PARTICLES Time constants (A) and steady-state activation and inactivation (B) as a function of the relative membrane potential V for sodium activation m (solid line) and inactivation h (long dashed line) and potassium activation n (short, dashed line). The steady-state sodium inactivation h_{∞} is a monotonically decreasing function of V , while the activation variables n_{∞} and m_{∞} increase with the membrane voltage. Activation of the sodium and potassium conductances is a much steeper function of the voltage, due to the power-law relationship between the activation variables and the conductances. Around rest, G_{Na} increases e -fold for every 3.9 mV and G_K for every 4.8 mV. Activating the sodium conductance occurs approximately 10 times faster than inactivating sodium or activating the potassium conductance. The time constants are slowest around the resting potential.

(from Koch)

Simulation of membrane action potential:

The complete Hodgkin-Huxley model is a parallel-conductance model incorporating:

- nonlinear (active) potassium and sodium currents:

$$I_K = \bar{g}_K n^4 (V_m - E_K)$$

$$I_{Na} = \bar{g}_{Na} m^3 h (V_m - E_{Na}),$$

- a linear (passive) “leakage” current:

$$I_L = g_L (V_m - E_L), \quad (3.41)$$

- and a capacitive current: $I_C = C \frac{dV_m}{dt}$.

Simulation of membrane action potential (cont.):

In the case of the an injected depolarizing current I_d , the membrane equation is:

$$I_K + I_{Na} + I_L + C \frac{dV_m}{dt} = I_d. \quad (3.39)$$

With the equations describing the gating particle dynamics, we have one first-order nonlinear differential equation coupled with three first-order linear differential equations.

Analytical solutions are not very tractable, so in most cases it is necessary to find numerical solutions.

Simulation of membrane action potential (cont.):

- Hodgkin and Huxley had assistants doing numerical solutions by hand – not much fun!
- Matlab has a set of numerical ODE solvers.
- Software packages for simulating neurons include:
 - [HHsim: Graphical Hodgkin-Huxley Simulator](#)
 - [NEURON: For computer simulations of neurons and neural networks](#)
 - [The GEneral NEural Simulation System \(GENESIS\)](#)

Simulation of membrane action potential (cont.):

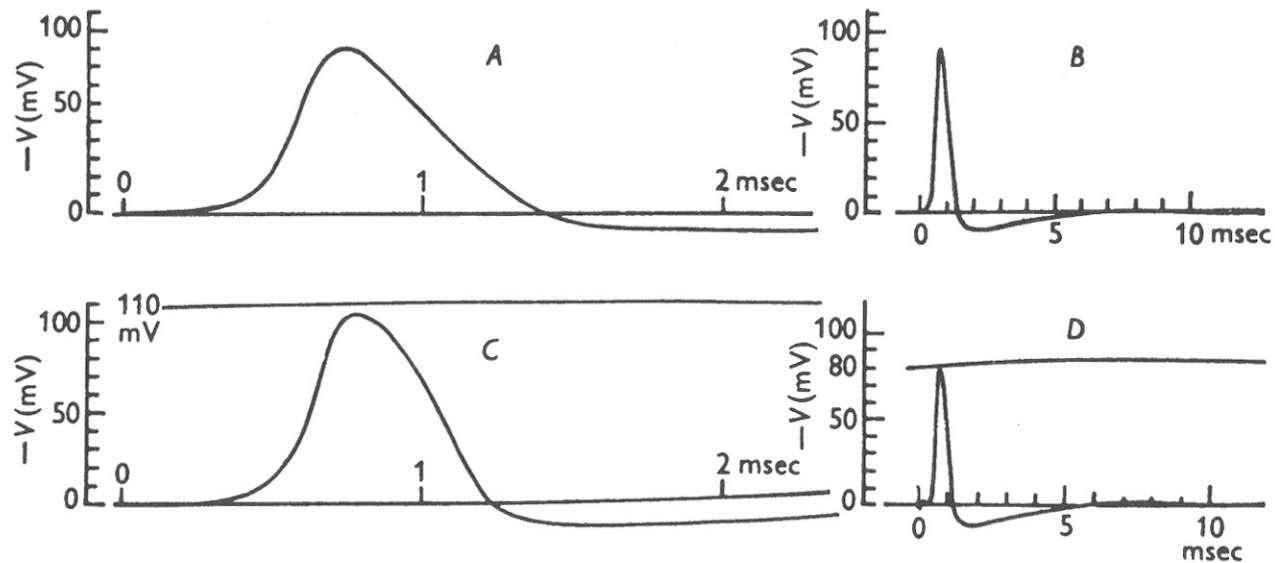


Figure 5.14. Curve A is the computed (propagated) action potential. Curve B is the same result to a slower time scale. Curves C and D are measured from different axons. [From A. L. Hodgkin and A. F. Huxley, A quantitative description of membrane current and its application to conduction and excitation in nerve, *J. Physiol.* 117:500–544 (1952).]

Action potential characteristics:

The characteristics of action potentials can be interpreted in terms of:

- how the ionic and capacitive currents vary as a function of time, membrane potential and injected current,

The behaviour of the ionic currents is understood in terms of:

- voltage-dependent channel gating, i.e., the dynamics of activation and inactivation particles.

Action potential characteristics (cont.):

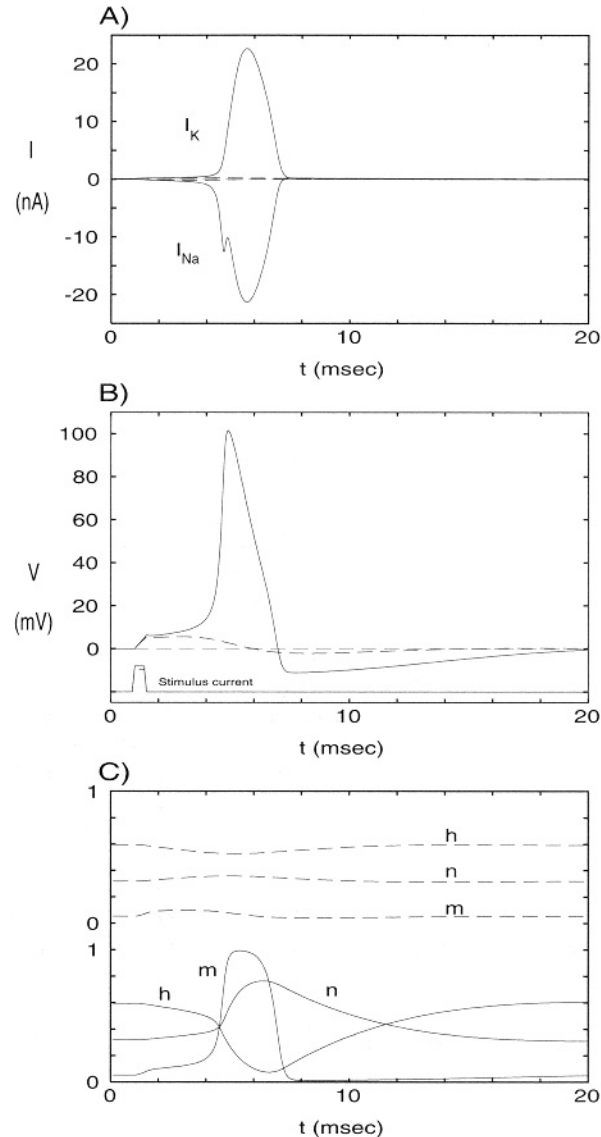


Fig. 6.5 HODGKIN-HUXLEY ACTION POTENTIAL Computed action potential in response to a 0.5-msec current pulse of 0.4-nA amplitude (solid lines) compared to a subthreshold response following a 0.35-nA current pulse (dashed lines). **(A)** Time course of the two ionic currents. Note their large sizes compared to the stimulating current. **(B)** Membrane potential in response to threshold and subthreshold stimuli. The injected current charges up the membrane capacity (with an effective membrane time constant $\tau = 0.85$ msec), enabling sufficient I_{Na} to be recruited to outweigh the increase in I_K (due to the increase in driving potential). The smaller current pulse fails to trigger an action potential, but causes a depolarization followed by a small hyperpolarization due to activation of I_K . **(C)** Dynamics of the gating particles. Sodium activation m changes much more rapidly than either h or n . The long time course of potassium activation n explains why the membrane potential takes 12 msec after the potential has first dipped below the resting potential to return to baseline level.

(from Koch)

Threshold behaviour:

Consider the case where the membrane is at rest and is then depolarized very rapidly to a relative membrane potential of v_m . If sodium activation is assumed to occur instantaneously and sodium inactivation and potassium activation are assumed to remain unchanged, then the net ionic current is:

$$\begin{aligned} I_0(v_m) &= \bar{g}_{\text{Na}} m^3(v_m) h(0) (v_m - E_{\text{Na}}) \\ &+ \bar{g}_{\text{K}} n^4(0) (v_m - E_{\text{K}}) \\ &+ g_L (v_m - E_L). \end{aligned} \quad (\text{Koch 6.21})$$

Threshold behaviour (cont.):

The resulting current-voltage relationship, shown below, explains the threshold behaviour of such a depolarization.

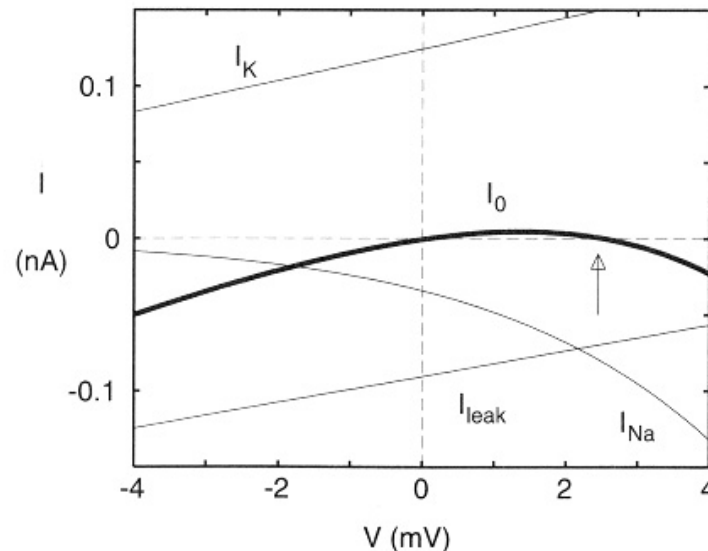


Fig. 6.6 CURRENT-VOLTAGE RELATIONSHIP AROUND REST Instantaneous $I-V$ relationship, I_0 , associated with the standard patch of squid axon membrane and its three components: $I_0 = I_{Na} + I_K + I_{leak}$ (Eq. 6.21). Because m changes much faster than either h or n for rapid inputs, we computed G_{Na} and G_K under the assumption that m adapts instantaneously to its new value at V , while h and n remain at their resting values. I_0 crosses the voltage axis at two points: a stable point at $V = 0$ and an unstable one at $V_{th} \approx 2.5$ mV. Under these idealized conditions, any input that exceeds V_{th} will lead to a spike. For the “real” equations, m does not change instantaneously and nor do n and h remain stationary; thus, I_0 only crudely predicts the voltage threshold which is, in fact, 6.85 mV for rapid synaptic input. Note that I_0 is specified in absolute terms and scales with the size of the membrane patch.

(from Koch)

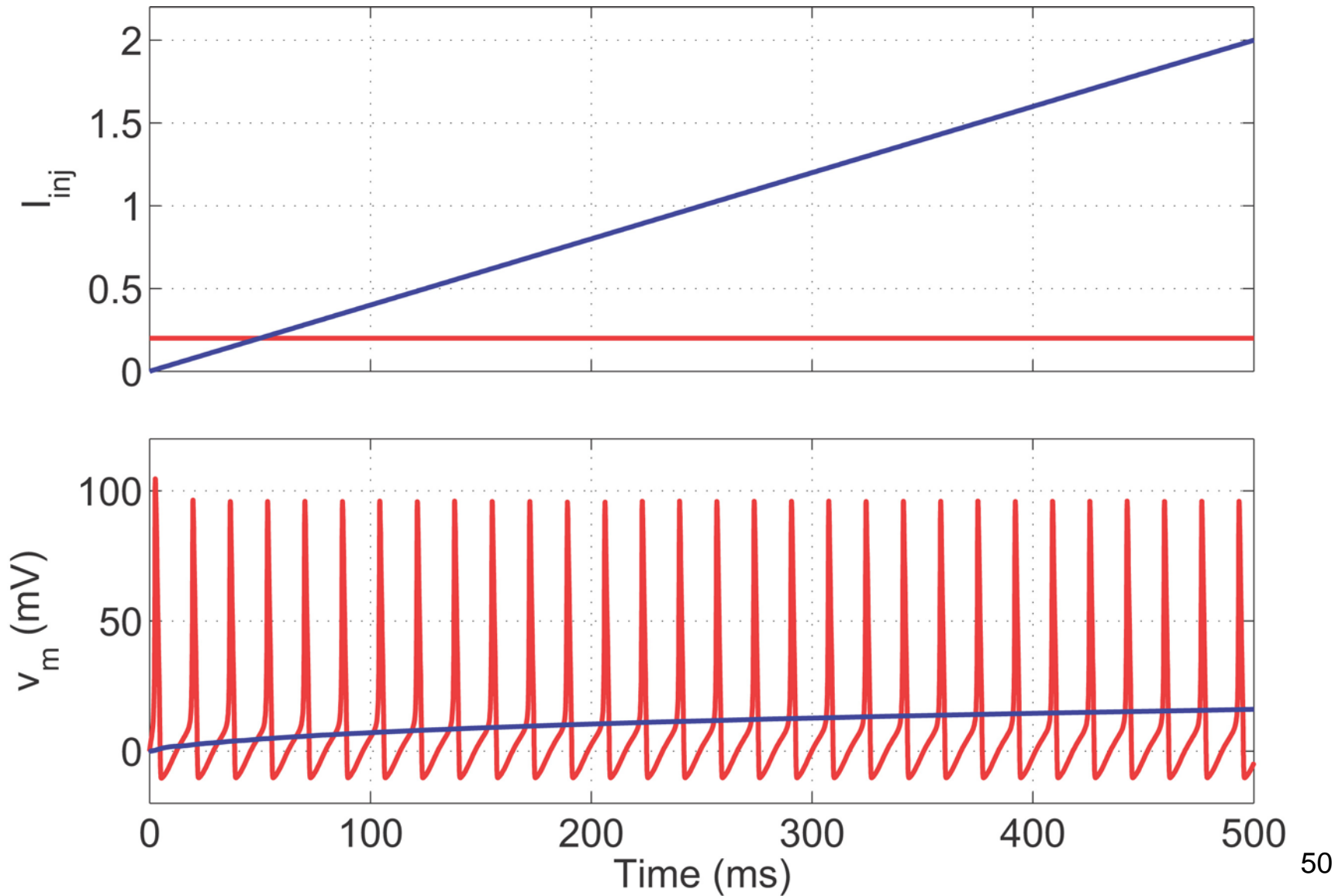
Accommodation:

Very slow changes in the membrane potential allow sodium inactivation and potassium activation to overcome sodium activation.

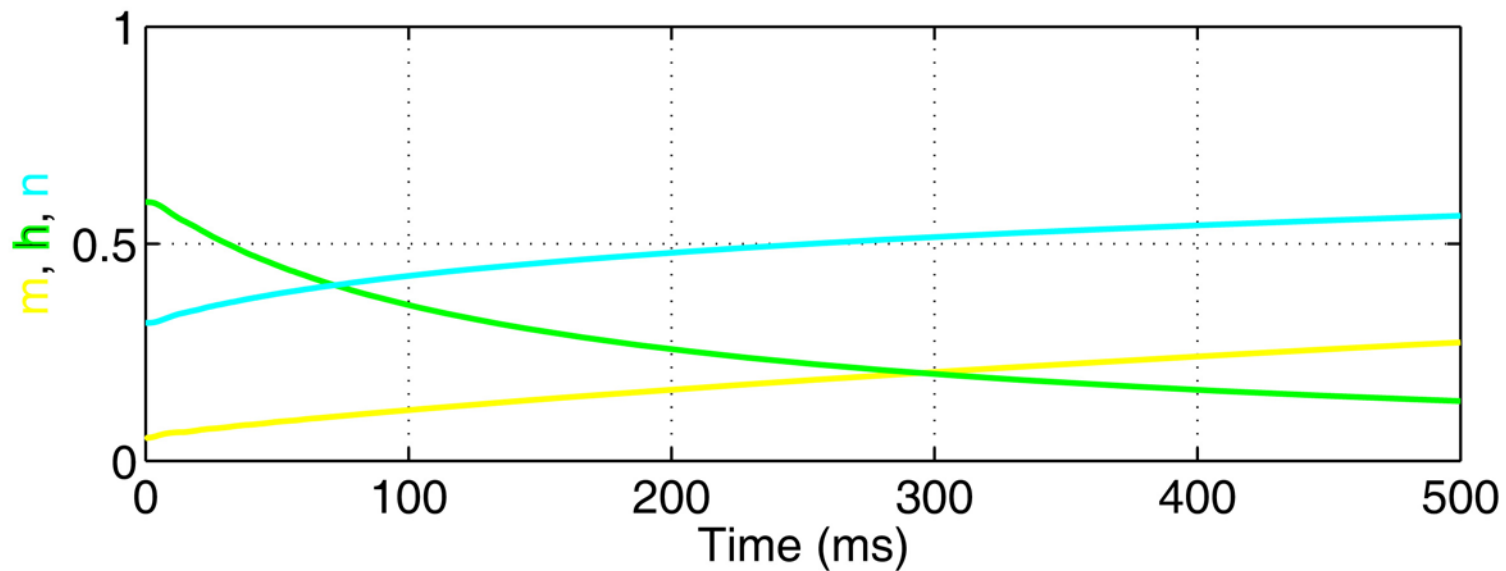
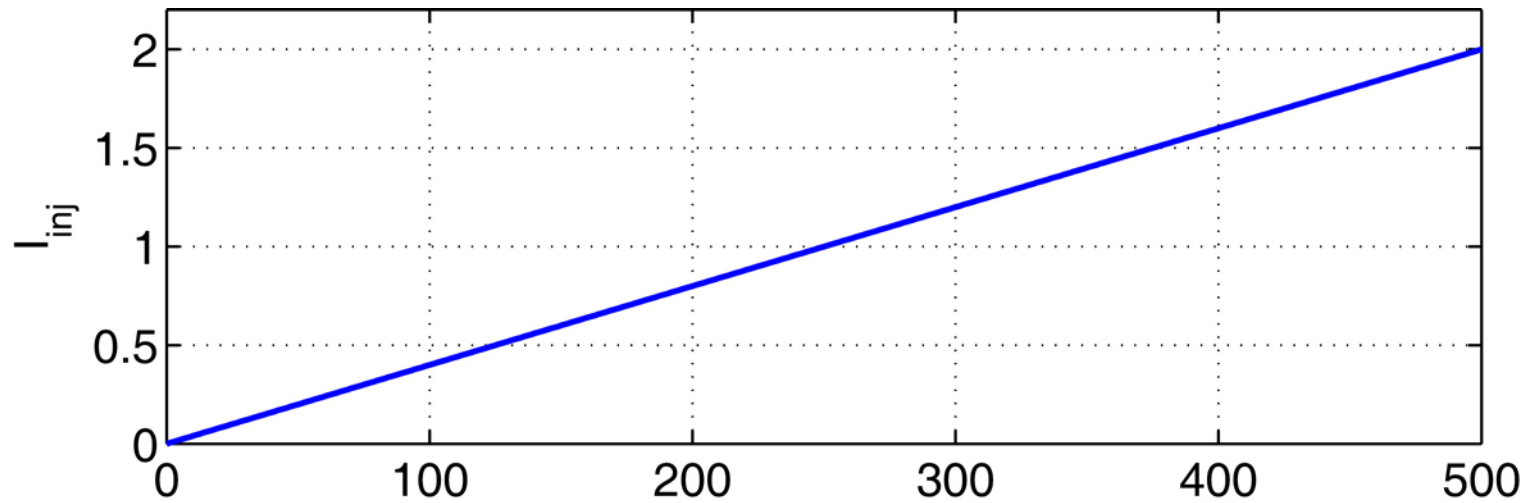
Consequently, the cell may not spike, even though the nominal threshold potential (i.e., in the case of a rapid depolarization) has been reached.

Any definition of a “threshold potential” is therefore restricted to a particular stimulus.

Accommodation (cont.):



Accommodation (cont.):



Strength-duration behaviour:

For a finite-duration current pulse, the strength of the stimulating current required to just elicit one action potential is characterized by a *strength-duration curve*.

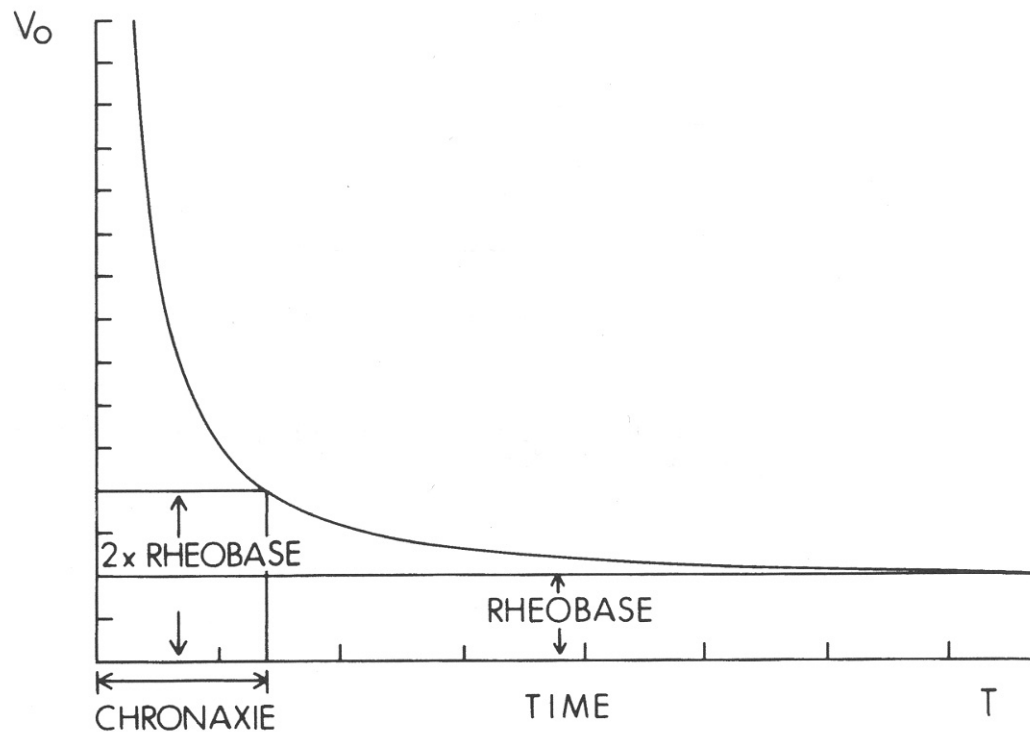


Figure 7.3. Strength-duration curve [from Eq. 7.5].

Anode break excitation:

Sodium deinactivation and potassium deactivation can give rise to an action potential at the offset of a hyperpolarizing pulse. This is referred to as “*anode break*” excitation.

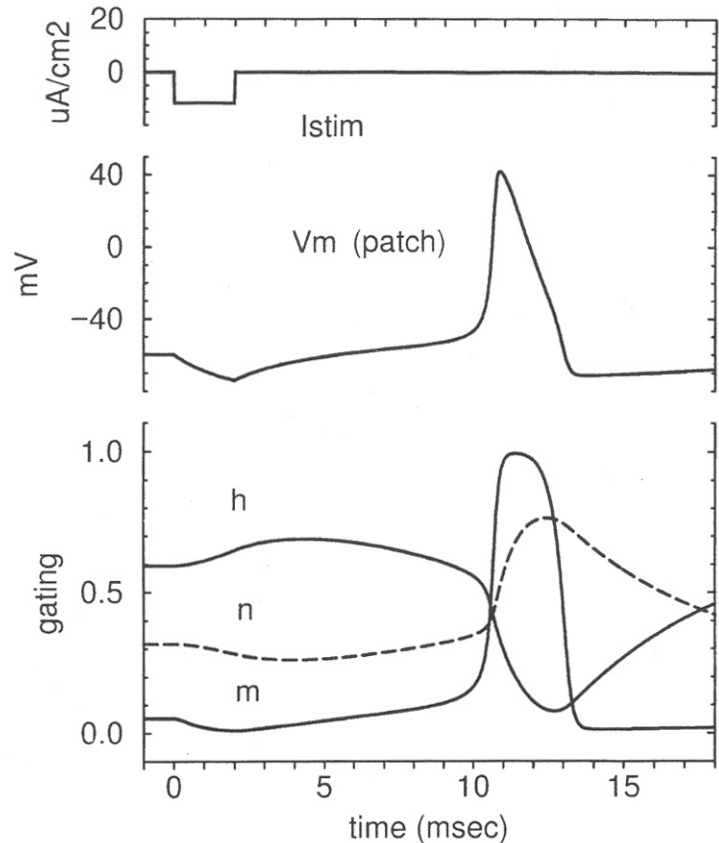


Figure 5.17. Anode break excitation. Computed values of m , n , h , and V_m from Hodgkin–Huxley equations. Space-clamped conditions. Values are computed during and after a 2 msec–11.7 $\mu A/cm^2$ hyperpolarizing pulse which starts at $t = 0$. The resting potential is -60 mV and the temperature is $T = 6.3^\circ C$.

Repetitive firing:

Injection of a sustained suprathreshold current gives rise to repetitive firing, illustrating the regenerative nature of spiking.

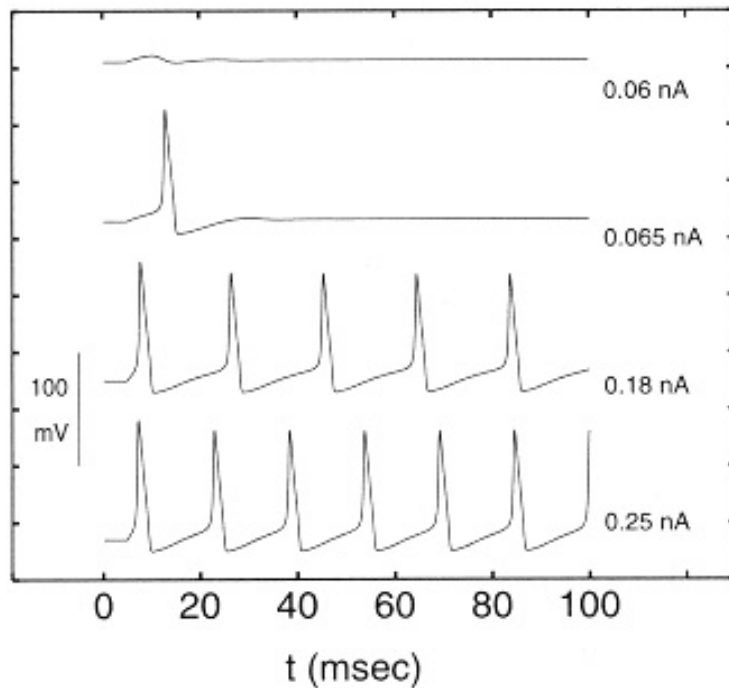


Fig. 6.8 REPETITIVE SPIKING Voltage trajectories in response to current steps of various amplitudes in the standard patch of squid axonal membrane. The minimum sustained current necessary to initiate a spike, termed *rheobase*, is 0.065 nA. In order for the membrane to spike indefinitely, larger currents must be used. Experimentally, the squid axon usually stops firing after a few seconds due to secondary inactivation processes not modeled by the Hodgkin–Huxley equations (1952d).

(from Koch)

Repetitive firing (cont.):

Increasing the injected current produces a slight increase in the spike rate.

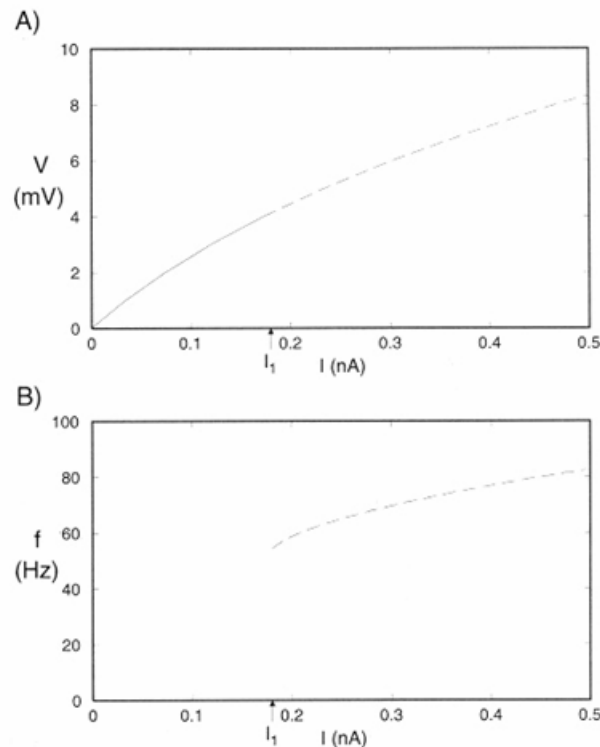


Fig. 6.9 SUSTAINED SPIKING IN THE HODGKIN-HUXLEY EQUATIONS (A) Steady-state I - V relationship and (B) f - I or discharge curve as a function of the amplitude of the sustained current I associated with the Hodgkin-Huxley equations for a patch of squid axonal membrane. For currents less than 0.18 nA, the membrane responds by a sustained depolarization (solid curve). At I_1 , the system loses its stability and generates an infinite train of action potentials: it moves along a stable limit cycle (dashed line). A characteristic feature of the squid membrane is its abrupt onset of firing with nonzero oscillation frequency. The steady-state I - V curve can also be viewed as the sum of all steady-state ionic currents flowing at any particular membrane potential V_m .

(from Koch)

Refractory effects:

- During most of the falling phase of an action potential it is impossible to generate another action potential, irrespective of the magnitude of injected current. This is referred to as the *absolute refractory period*.
- For some time following an action potential the injected current required to reach threshold is greater than is necessary when the membrane is at rest. This is referred to as the *relative refractory period*.

Refractory effects (cont.):

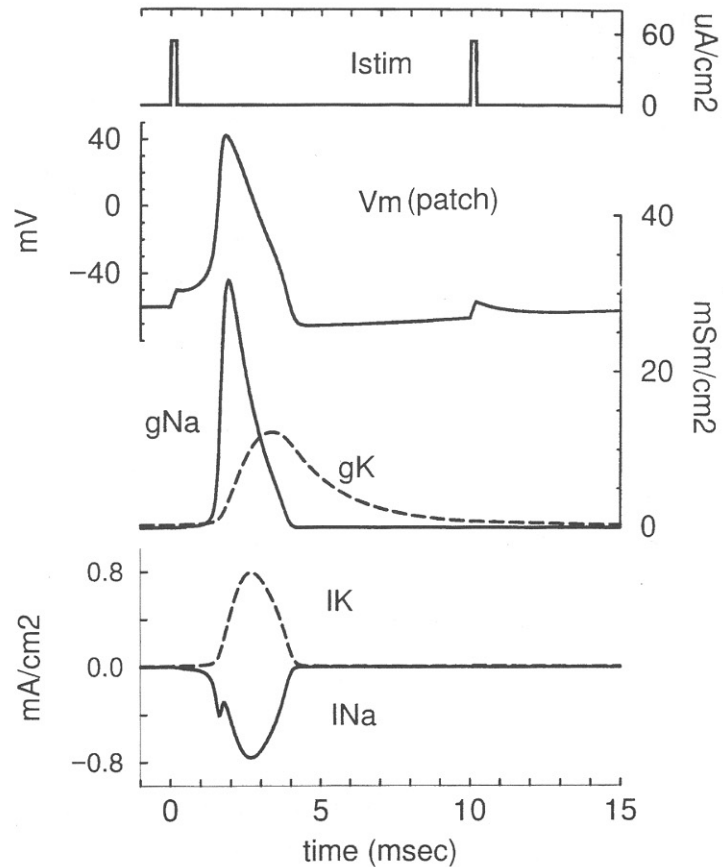


Figure 5.15. Calculated changes in membrane potential (upper curve), sodium and potassium conductances (middle curves), and sodium and potassium currents; all curves are for a squid giant axon membrane patch. The second stimulus is seen to elicit essentially no response even though it is of the same size and duration as the first (for which an action potential results, as is seen). It therefore identifies the condition as refractory. Since a larger stimulus would generate an action potential this is a *relatively refractory* period. The stimulus amplitude is $53 \mu A/cm^2$ and its duration is 0.2 msec. The second stimulus is similar in amplitude and duration and occurs after a delay of 15 msec. The resting potential is -60 mV while $T = 6.3^\circ C$. Calculations were based on the Hodgkin-Huxley equations.

Refractory effects (cont.):

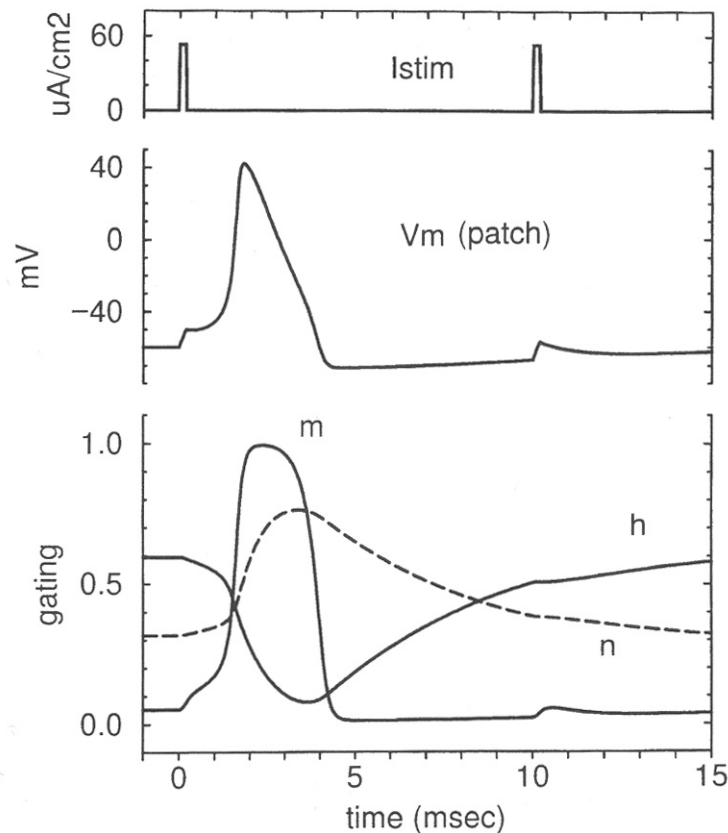


Figure 5.16. Computed membrane action potential using the Hodgkin–Huxley equations. In addition to the temporal variation of $V_m(t)$, the gating variables temporal behavior [i.e., $m(t)$, $n(t)$, $h(t)$] are shown. In this simulation resting $v_m = -60$ mV, while the stimulus current starting at $t = 0$ is $53 \mu A/cm^2$ for 0.2 msec. The temperature is $6.3^\circ C$.

Refractory effects (cont.):

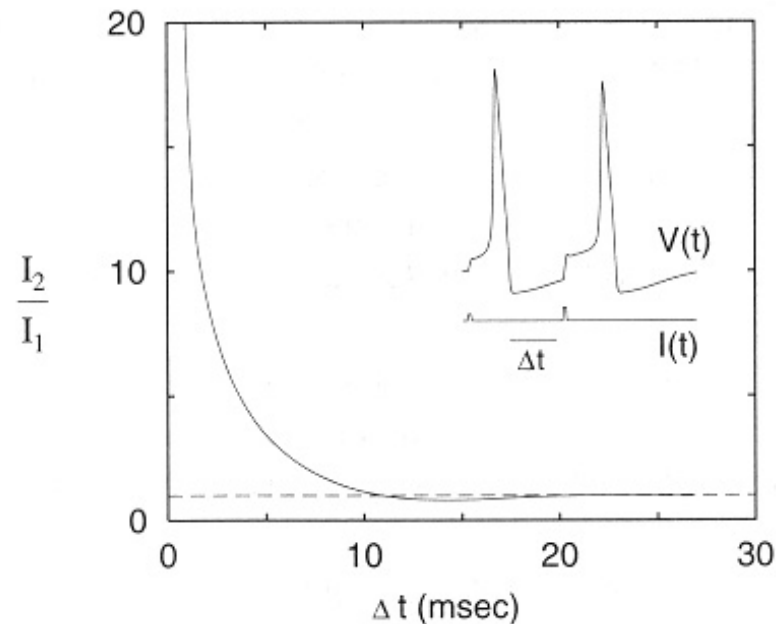


Fig. 6.7 REFRACTORY PERIOD A 0.5-msec brief current pulse of $I_1 = 0.4$ nA amplitude causes an action potential (Fig. 6.5). A second, equally brief pulse of amplitude I_2 is injected Δt msec after the membrane potential due to the first spike having reached $V = 0$ and is about to hyperpolarize the membrane. For each value of Δt , I_2 is increased until a second spike is generated (see the inset for $\Delta t = 10$ msec). The ratio I_2/I_1 of the two pulses is here plotted as a function of Δt . For several milliseconds following repolarization, the membrane is practically inexcitable since such large currents are unphysiological (*absolute refractory period*). Subsequently, a spike can be generated, but it requires a larger current input (*relative refractory period*). This is followed by a brief period of reduced threshold (*hyperexcitability*). No more interactions are observed beyond about $\Delta t = 18$ msec.

(from Koch)